AMERICAN SOCIETY FOR MICROBIOLOGY | Journal of Virology®

Human Adenovirus Core Protein V Is Targeted by the Host SUMOylation Machinery To Limit Essential Viral Functions

Nora Freudenberger,[a,b] Tina Meyer,[b] Peter Groitl,[a] Thomas Dobner,[b] Sabrina Schreiner[a]

[a]Institute of Virology, Technische Universität München/Helmholtz Zentrum München, Munich, Germany
[b]Heinrich Pette Institute, Leibniz Institute for Experimental Virology, Hamburg, Germany

ABSTRACT Human adenoviruses (HAdV) are nonenveloped viruses containing a linear, double-stranded DNA genome surrounded by an icosahedral capsid. To allow proper viral replication, the genome is imported through the nuclear pore complex associated with viral core proteins. Until now, the role of these incoming virion proteins during the early phase of infection was poorly understood. The core protein V is speculated to bridge the core and the surrounding capsid. It binds the genome in a sequence-independent manner and localizes in the nucleus of infected cells, accumulating at nucleoli. Here, we show that protein V contains conserved SUMO conjugation motifs (SCMs). Mutation of these consensus motifs resulted in reduced SUMOylation of the protein; thus, protein V represents a novel target of the host SUMOylation machinery. To understand the role of protein V SUMO posttranslational modification during productive HAdV infection, we generated a replication-competent HAdV with SCM mutations within the protein V coding sequence. Phenotypic analyses revealed that these SCM mutations are beneficial for adenoviral replication. Blocking protein V SUMOylation at specific sites shifts the onset of viral DNA replication to earlier time points during infection and promotes viral gene expression. Simultaneously, the altered kinetics within the viral life cycle are accompanied by more efficient proteasomal degradation of host determinants and increased virus progeny production than that observed during wild-type infection. Taken together, our studies show that protein V SUMOylation reduces virus growth; hence, protein V SUMOylation represents an important novel aspect of the host antiviral strategy to limit virus replication and thereby points to potential intervention strategies.

IMPORTANCE Many decades of research have revealed that HAdV structural proteins promote viral entry and mainly physical stability of the viral genome in the capsid. Our work over the last years showed that this concept needs expansion as the functions are more diverse. We showed that capsid protein VI regulates the antiviral response by modulation of the transcription factor Daxx during infection. Moreover, core protein VII interacts with SPOC1 restriction factor, which is beneficial for efficient viral gene expression. Here, we were able to show that core protein V also represents a novel substrate of the host SUMOylation machinery and contains several conserved SCMs; mutation of these consensus motifs reduced SUMOylation of the protein. Unexpectedly, we observed that introducing these mutations into HAdV promotes adenoviral replication. In conclusion, we offer novel insights into adenovirus core proteins and provide evidence that SUMOylation of HAdV factors regulates replication efficiency.

KEYWORDS human adenovirus, HAdV, protein V, core, SUMO, PML-NB, human adenovirus

Human adenoviruses (HAdV) show considerable tissue tropism, but the primary targets are terminally differentiated epithelial cells. This results in a broad spectrum of clinical symptoms with HAdV as the causative agent (1). Usually, an HAdV infection is mild and self-limiting. However, in rare cases the course of infection can be

Received 28 August 2017 **Accepted** 10 November 2017

Accepted manuscript posted online 22 November 2017

Citation Freudenberger N, Meyer T, Groitl P, Dobner T, Schreiner S. 2018. Human adenovirus core protein V is targeted by the host SUMOylation machinery to limit essential viral functions. J Virol 92:e01451-17. https://doi.org/10.1128/JVI.01451-17.

Editor Lawrence Banks, International Centre for Genetic Engineering and Biotechnology

Address correspondence to Sabrina Schreiner, sabrina.schreiner@tum.de.

severe. Worst affected by such complications are newborns or immunocompromised patients, e.g., those suffering from AIDS or having received an organ transplant (2). The latter group presents a serious problem since no specific treatment is yet available for adenoviral infections. Hence, the therapy during severe infection courses can only be symptomatic and not uncommonly results in the death of a patient.

Little structural information exists about the adenoviral core. It contains three highly basic proteins which bind the viral genome in a sequence-unspecific manner: the major core protein VII, the minor core protein V, and the small peptide μ (μ, or X) (3). All of them are encoded by distinct mRNAs of the L2 family (4).

Within all adenovirus genera, minor core protein V is specific for mastadenoviruses. It has a length of 368 amino acids (aa) with a calculated molecular mass of 41 kDa (5). Protein V is present in ~157 copies per virion and is speculated to bridge the viral core with the surrounding capsid through its interaction with capsid protein VI (5). Moreover, early cross-linking studies indicated that protein V exists in a complex with VII, μ, or both proteins together; VII and μ could not be detected in complexes without V (5). It was further shown that protein V is able to dimerize in solution (6). Based on these findings, a model was proposed for the stoichiometric adenosome (nucleosome-like state of the viral genome) organization where the viral DNA wraps around six molecules of protein VII, which are interspaced by one molecule of protein V. However, the position of protein μ in this condensed DNA structure remains elusive (3). Complexes between protein V and DNA have been shown to be very stable. Due to its ability to facilitate interactions between the other core proteins and the viral genome, protein V is speculated to have functions similar to those of cellular histone 1 (H1) (6).

So far, no functional domains have been identified within the primary sequence of protein V. However, it contains several regions that target the protein to the nucleus (NLS) as well as to the nucleolus (NoLS) of infected host cells. The N-terminal motif (aa 23 to 78) and the C-terminal motif (aa 315 to 337) target the protein to the nucleoli as well as to the nucleoplasm independently of each other. In contrast, the central NLS can only mediate localization of protein V in the nucleoplasm (7). Indeed, newly synthesized protein V is found exclusively in the nucleus during HAdV infection where it also colocalizes with nucleoli but spares adenoviral replication centers (7). Protein V was found to induce the relocalization of two major nucleolar proteins, nucleolin (C23) and nucleophosmin (B23/NPM1), to the cytoplasm during transfection experiments (7).

Several studies investigated the behavior of incoming protein V within the first hours of HAdV infection. Predominantly performed at a high multiplicity of infection (MOI), the studies agree on a rapid transport of protein V to the host nucleus, where it immediately partially associates with nucleoli (8). However, Puntener and coworkers claim that protein V does not enter the nucleus early after infection. They propose that it dissociates in two sequential steps. The first fraction of protein V is released from the viral particle when it is released from an endosome to the cytoplasm. This process is assumed to be associated with the disassembly of the capsid vertices. The second fraction of protein V is released during final capsid uncoating at the nuclear pore complex (NPC) and could not be observed inside the nucleus afterwards. Consequently, the viral genome translocation is proposed to follow in a complex with core protein VII but not with protein V (9). Regarding the latter step, Hindley and coworkers came to a similar conclusion. However, they could detect protein V in the nucleus at early time points after adenovirus infection and concluded that protein V is able to enter the nucleus independently of the viral DNA/protein VII complex (10). As an incoming virion protein present in the infected host cell after entry into the host nucleus, protein V could have a yet unknown regulatory influence on establishing conditions favorable for the onset of viral replication. Furthermore, it is a late-phase protein, which might not only be packed into new infectious particles but also play a part in regulation of virion assembly. However, the last steps of adenoviral infections comprising assembly, encapsidation, maturation, and escape of viral progeny and also the role of protein V during the immediate early phase are still not understood in detail.

PML nuclear bodies (PML-NBs) are nuclear, spherical multiprotein complexes located

in the interchromosomal space, where they are tightly bound to the nuclear matrix (11). Many of the processes associated with PML-NBs are linked to a posttranslational modification (PTM) of the proteins involved, called SUMO. "SUMO" is short for small ubiquitin-like modifier since the protein shares around 18% sequence similarity with ubiquitin and is covalently bound to its target proteins in a mechanistically comparable manner. In contrast to SUMO1, SUMO2 and SUMO3 (SUMO2/3) proteins are able to form polymeric chains since they contain a conserved acceptor lysine residue within their sequence (12). The attachment of SUMO proteins to their targets occurs in a reversible three-step enzymatic cascade. PML-NBs have been discussed as nuclear sites for PTM themselves and especially represent hotspots for SUMO modification. All enzymes involved in SUMOylation or deSUMOylation of proteins are present at the PML-NBs, and PML has been proposed to have an E3 SUMO ligase activity (13).

Here, we show that protein V indeed represents a novel target of the host SUMO machinery and partially localizes to PML nuclear domains. Remarkably, after blocking protein V SUMOylation by site-directed mutagenesis, we saw a beneficial effect on viral gene expression and replication processes. Biochemical analyses revealed that a block of protein V SUMO conjugation promotes viral DNA synthesis and coordinates nucleolus association during productive infection.

Further functional studies of adenoviral structural proteins such as protein V would contribute to a profound understanding of the complex processes mentioned above and pave the way toward developing novel antiviral intervention strategies.

RESULTS

HAdV protein V partially colocalizes with host nucleoli. Protein V accumulates at the nucleoli of infected cells as well as diffusely in the nucleoplasm (7, 8). Our results confirm protein V proteins in the nuclei of infected cells (Fig. 1A). In 90% of the analyzed cells ($n = 40$), protein V revealed nuclear accumulations (Fig. 1A, frame f), colocalizing with nucleophosmin (B23), a cellular marker of nucleoli (14) (Fig. 1A, frames e and g). By using the Fiji plug-in Colocalization Threshold, analysis of pixel intensities within nucleolar regions and their direct surrounding area resulted in a linear correlation of the red- and green-channel pixels, with the gradient reflecting the ratio of their intensities (Fig. 1A). The plug-in uses an auto-threshold determination using the Costes method, and the proportion of a signal in one channel that colocalizes with the signal in the other channel is reflected by the thresholded Mander's correlation coefficients (tM). The tM ranges from 0 to 1, where 0 means no colocalization and 1 means perfect colocalization of signal intensities. The tM values in Fig. 1A average the signal correlation in all nucleolar regions of one picture. This amounts to a tM1 of 0.94 (green) and tM2 of 0.90 (red) for frames f and g, respectively. Accordingly, accumulation of adenoviral protein V at the host nucleoli could be confirmed in HepaRG cells. In addition, we also found smaller nuclear protein V-containing dots (Fig. 1A, frame f), indicating association with other host nuclear domains, such as PML-NBs.

We further elucidated whether this adenoviral core protein is conjugated with SUMO proteins. We transfected either a Flag- or hemagglutinin (HA)-tagged V-expressing plasmid and observed an additional band between 55 and 70 kDa (Fig. 1B, left panel, lane 2), matching the size of a conjugated SUMO protein. Furthermore, a smear of Flag-V protein toward higher molecular masses was detected, which is typical for the formation of SUMO or ubiquitin chains. Similarly, HA-V shows discrete slower-migrating bands, matching the size of polySUMOylation (Fig. 1B, right panel, lane 2). An even faster migrating form was found at 35 kDa (Fig. 1B, right panel, lane 2), indicating an as yet unknown, C-terminally shortened isoform of HAdV protein V or protein degradation.

HAdV protein V is covalently modified with SUMO proteins. To validate protein V PTM SUMOylation, a Flag-V-expressing plasmid was transiently transfected into cells stably expressing 6His-tagged SUMO1 or 6His-tagged SUMO2 (12) prior to Ni-nitrilotriacetic acid (NTA) purification (Fig. 2A). Our data show that SUMO2 chains are conjugated with the viral core protein V (Fig. 2A, left panel, lane 6). Additionally, the protein itself, migrating at a size of 50 kDa, is pulled down, indicating an unspecific

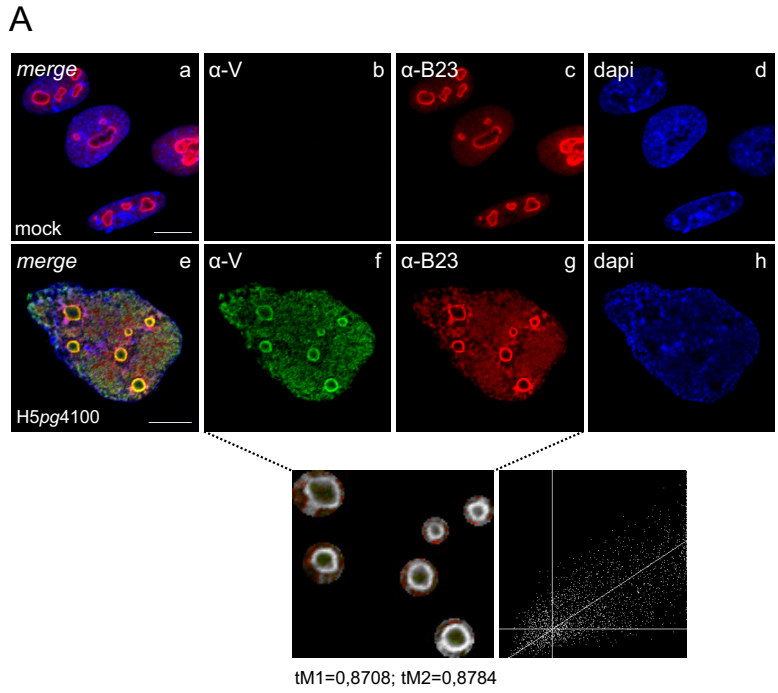

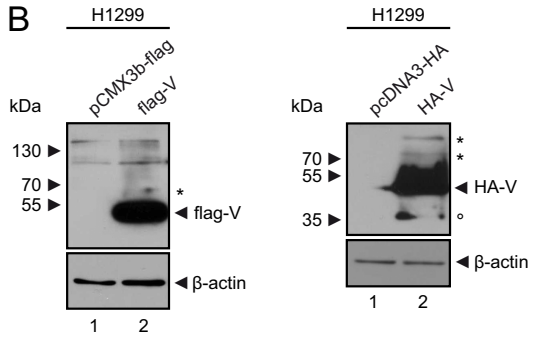

FIG 1 HAdV protein V association with host nucleoli structures. (A) HepaRG cells were infected with H5*pg*4100 (MOI of 20) and fixed with 4% PFA at 24 h p.i. Mock, uninfected control. Proteins were detected with pAb anti-protein V and MAb FC-61991 (anti-B23). Primary antibodies were detected with secondary antibodies conjugated with Alexa 488 (green) or Cy3 (red), and nuclei were stained with DAPI (blue). Merged images show the overlay of single images of each row. Images were captured with a Nikon confocal fluorescence microscope. Below these images, colocalization of adenoviral protein V and B23 at host nucleoli is depicted by two-dimensional histograms, which correlate the pixel intensities of two channels and show the corresponding channel overlay of the analyzed regions of interest. tM is the thresholded Mander's split coefficient, and the number indicates the channel, with 1 corresponding to the red channel (B23) and 2 corresponding to the green channel (protein V). (B) H1299 cells were transfected with either 10 μg of an empty vector control, a pCMX3b-Flag-V expression plasmid (left panel), or a pcDNA3-HA-V expression plasmid. Cells were harvested at 48 h p.t. Total cell lysates were resolved by SDS-PAGE and visualized by immunoblotting. Levels of Flag-V and HA-V were detected by using MAb M2 (anti-Flag) and MAb 3F10 (anti-HA); input levels of β-actin were detected by using MAb AC-15 (anti-β-actin). Molecular masses in kilodaltons are indicated on the left, while corresponding proteins are labeled on the right.

interaction of a Flag-V fraction with the Ni-NTA matrix (Fig. 2A, lanes 4 and 6). Modification of protein V with SUMO1 cannot be ruled out since protein V expression is low compared to that in SUMO2-expressing cells (Fig. 2A, right panel, lanes 4 to 6).

Next, we superinfected cells transiently expressing Flag-V and analyzed SUMOylation of the viral core protein. Our result showed that protein V SUMOylation is weaker in 6His-SUMO2 HeLa cells with protein V expressed from the viral genome during infection than in cells transiently overexpressing Flag-V (Fig. 2B, left panel, lanes 6 to 8).

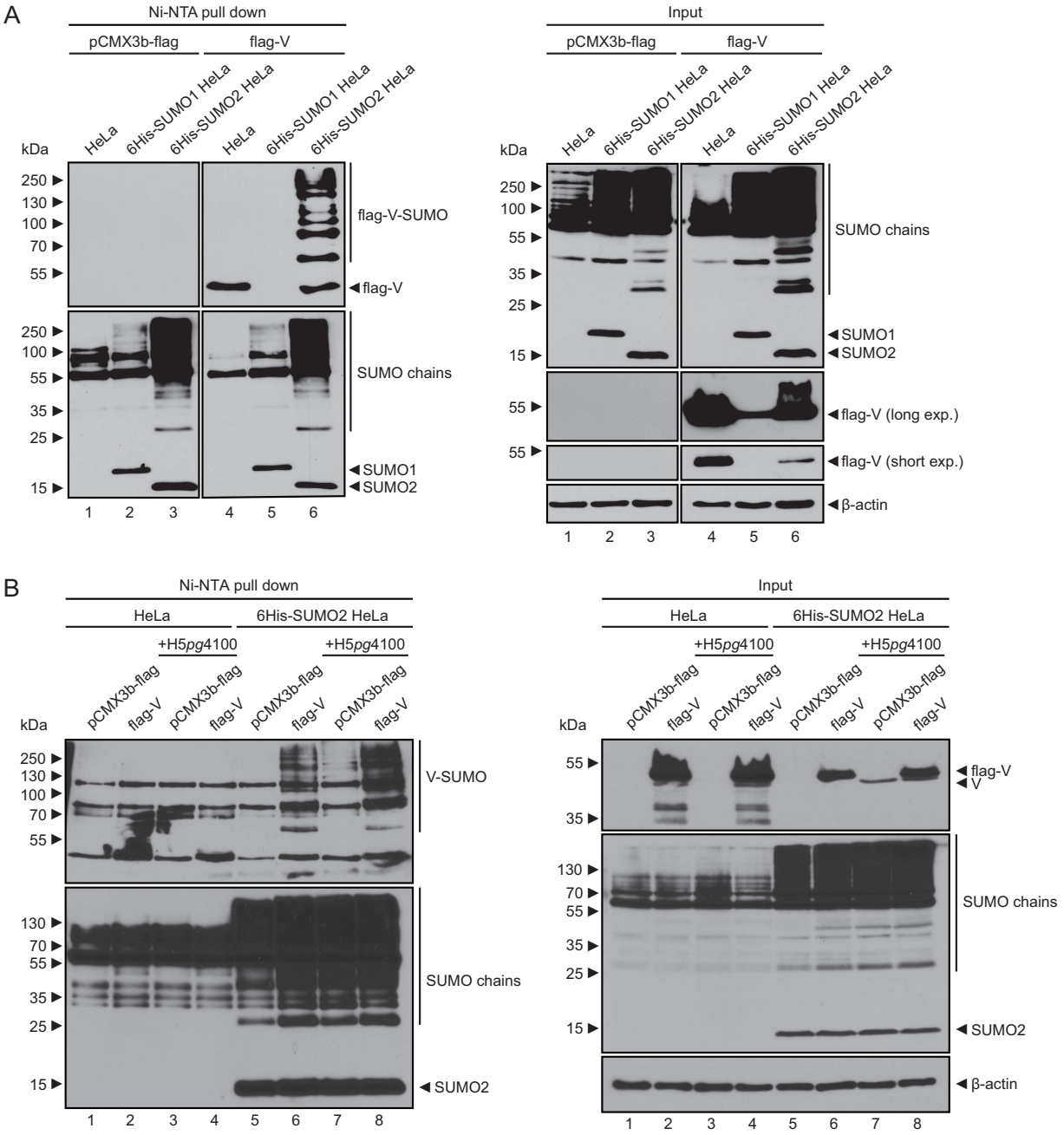

FIG 2 Protein V is a novel SUMO target in the host cell. (A) HeLa cells and HeLa cells stably expressing 6His-SUMO1 or 6His-SUMO2 were transfected with 10 μg of an empty vector control or pCMX3b-Flag-V expression plasmid, harvested at 48 h p.t., and subjected to a guanidinium chloride buffer. 6His-SUMO conjugates were purified using a Ni-NTA matrix (Ni-NTA pulldown), and input represents total cell lysates. Samples were separated by SDS-PAGE and visualized by immunoblotting. Ni-NTA-purified and input proteins were detected using MAb M2 (anti-Flag), MAb anti-6His, and MAb AC-15 (anti-β-actin). Molecular masses in kilodaltons are indicated on the left, while corresponding proteins are labeled on the right (exp., exposure). (B) HeLa cells or HeLa cells stably expressing 6His-SUMO2 were transfected with 10 μg of an empty vector control or pCMX3b-Flag-V expression plasmid and superinfected with H5*pg*4100 (MOI of 20) at 24 h p.t. The cells were harvested at 24 h p.i. and subjected to a guanidinium chloride buffer. 6His-SUMO conjugates purified by Ni-NTA pulldown, and input total cell lysates were resolved by SDS-PAGE and visualized by immunoblotting. Ni-NTA-purified and input proteins were detected using pAb anti-V, MAb anti-6His, and MAb AC-15 (anti-β-actin). Molecular masses in kilodaltons are indicated on the left, while corresponding proteins are labeled on the right.

However, 6His-SUMO2 HeLa cells superinfected and overexpressing Flag-V reveal efficient protein V SUMOylation (Fig. 2B, lanes 6 and 8).

Identification of several putative protein V SCMs. Since we had observed protein V SUMO conjugation, we performed an *in silico* analysis of the viral protein to identify putative SUMO conjugation and/or SUMO-interacting motifs (SCMs and/or SIMs, re-

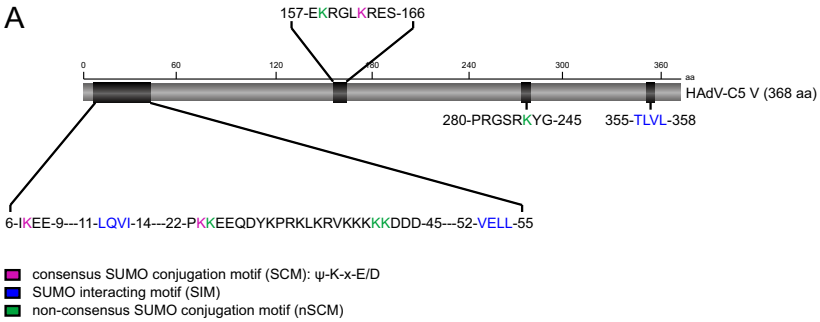

B

SUMO-motif	K→R-exchange	designation
6-IKEE-9	6-IREE-9	HAdV-C5 VK7R
22-PKKEE-26	22-PRREE-26	HAdV-C5 VK23/24/R
161-LKRE-164	161-LRRE-164	HAdV-C5 VK162R
K7+K23/24	R7+R23/24	HAdV-C5 VK7/23/24R
K23/24+K162	R23/24+R162	HAdV-C5 VK23/24/162R
K7+K162	R7+R162	HAdV-C5 VK7/162R
K7+K23/24+K162	R7+R23/24+R162	HAdV-C5 V4xKR

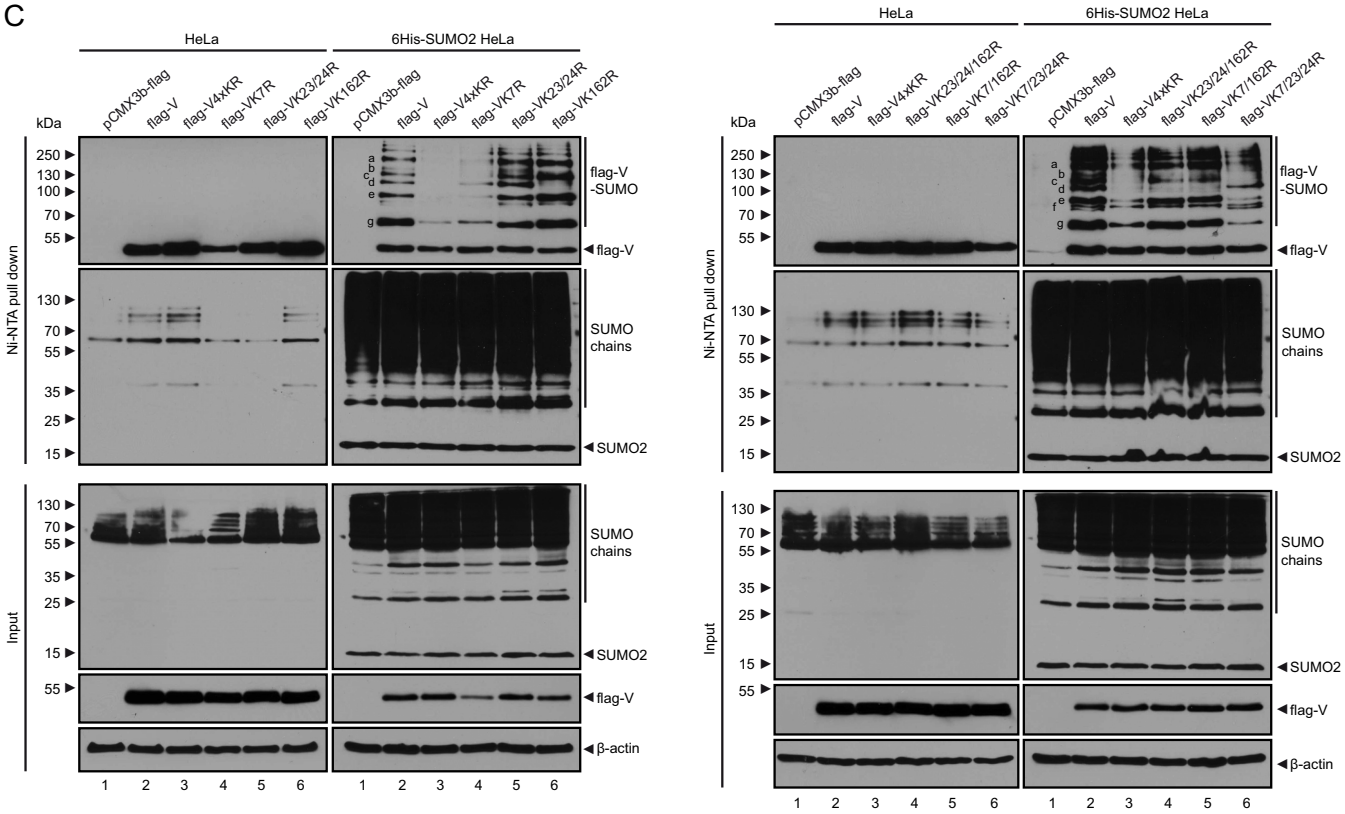

FIG 3 Identification of protein V SUMOylation sites. (A) *In silico* analysis of protein V to determine potential SUMO conjugation or interaction motifs, using the algorithms SUMOPlot (Abgent, Inc., San Diego, CA), GPS-SUMO, and Jassa. (B) Schematic illustration of the protein V SCM mutants used in the experiments. SCMs are depicted in pink, nSCMs are in green, and K → R exchanges are in yellow. (C) HeLa cells or HeLa cells stably expressing 6His-SUMO2 were transfected with either 10 μg of an empty vector control, pCMX3b-Flag-V expression plasmid, or Flag-V SCM mutants as indicated. Cells were harvested at 48 h p.t. and subjected to a guanidinium chloride buffer. 6His-SUMO conjugates purified by using Ni-NTA pulldown and input of total cell lysates were resolved by SDS-PAGE and visualized by immunoblotting. Ni-NTA-purified and input proteins were detected using MAb M2 (anti-Flag), MAb anti-6His, and MAb AC-15 (anti-β-actin). Molecular masses in kilodaltons are indicated on the left, while corresponding proteins are labeled on the right.

spectively) (Fig. 3A). All algorithms used indicated three consensus SCMs of high probability within V: K7, K23, and K162 (Fig. 3A and B, depicted in pink). Additionally, one nonconsensus SUMO conjugation site (nSCM) was predicted with high probability at residue K24, and several nSCMs with low or medium probabilities were found (Fig. 3A, depicted in green). Furthermore, three SIMs were predicted within protein V although they have low probability and appear only with the use of low thresholds (Fig. 3A, depicted in blue).

Based on these findings, different putative SCM mutants of HAdV protein V were generated by site-directed mutagenesis to determine the actual sites of protein V SUMOylation. The coding sequence of protein V was modified to replace the lysine residue within the motif with arginine. This retains the local as well as the net charge

of the protein and thereby reduces the possibility of conformational changes, which could cause a change or even a loss of function. To obtain these mutants, single nucleotides of the protein V coding sequence were exchanged by quick-change PCR using the Flag-V expression plasmid as a template. Since this results in a lysine-to-arginine exchange within the primary protein sequence of protein V (Fig. 3B, depicted in yellow), the mutants were named VK7R and VK162R. In the case of the third SCM, containing K23, the neighboring K24, which was predicted with low probability as an nSCM, was also replaced, leading to a double mutant named VK23/24R. Additional plasmids were generated with only one intact SCM left within protein V (VK7/23/24R, VK23/24/162R, and VK7/162R). V4×KR has alterations in all three SCMs and the nSCM containing K24 (Fig. 3B).

The influence of these SCM mutations on protein V SUMOylation was investigated in transfected HeLa or 6His-SUMO2 HeLa cells, which were prepared for Ni-NTA purification at 48 h posttransfection (p.t.). Intriguingly protein V4×KR showed severely reduced SUMO modification (Fig. 3C, lane 3). In contrast, the single SCM mutants, apart from protein VK7R, do not show such strong alteration of SUMO2 modification (Fig. 3C, left panel, lanes 4 to 6). The pattern of Flag-tagged protein VK23/24R is identical to that of Flag-protein V (Fig. 3C, left panel, lanes 2 and 5), whereas Flag-tagged protein VK162R lacks certain bands (b and d) although the overall signal of the other bands is even stronger than those of the wild-type (wt) protein (Fig. 3C, left panel, lanes 2 and 6). Interestingly, Flag-tagged protein VK7R shows a reduction of SUMO2 modification almost as strong as that of protein V4×KR although the amount of pulled down SUMO conjugates is slightly higher than that for protein V (Fig. 3C, left panel, lanes 2 to 4). This indicates a major role of lysine residue K7 for the SUMO conjugation with protein V. It is noteworthy, however, that the input concentration of protein VK7R was reduced (Fig. 3C, left panel, lane 4). The protein V mutants with only one intact SCM were also compared to wt protein V and protein V4×KR (Fig. 3C, right panel). As a whole, the signal intensity of the Ni-NTA purification was stronger than that in the previous experiment, leading to the occurrence of a new double band for Flag-protein V at approximately 70 kDa (Fig. 3C, top right panel, lane 2, band f). This band can clearly be assigned to K162 since it is not visible if this residue is replaced by arginine (Fig. 3C, right panel, lanes 2 to 6). The same is true for SUMO band d (Fig. 3C, right panel, lanes 4 to 6), which matches the result of the previous experiment (Fig. 3C, left panel, lanes 4 to 6). In contrast to results of the previous experiment, it does not make a difference whether K7 or K23/24 is exchanged. If one site is still intact, the pattern of SUMO2 modification is identical (Fig. 3C, right panel, lanes 4 and 5). Hence, each residue seems to be able to compensate for the lack of the other, indicating that the drastic reduction of protein VK7R SUMOylation (Fig. 3C, left panel, lanes 2 to 4) results, rather, from its low protein concentration. If both conjugation sites are missing and only SCM K162 is present, band c disappears (Fig. 3C, right panel, lane 6). Additionally, bands a, e, and g are less intense, indicating a greater dependence of these SUMO signals on K7, K23, and K24 than on K162 (Fig. 3C, right panel, lanes 3 to 6). Band b is not clearly visible in all of the protein V SCM mutants (Fig. 3C, right panel, lanes 3 to 6). The combination of these observations results in the SUMO2 pattern of protein V4×KR where four SUMO bands (b to d and f) are no longer detectable, and the others are reduced (Fig. 3C, left panel, lanes 2 to 3). Taken together, the results indicate that only two bands of the protein V SUMO2 pattern can be precisely assigned to a certain SCM, i.e., d and f belonging to K162. Remarkably, protein V still shows SUMO2 modification, although significantly reduced, if all of its SCMs are altered (Fig. 3C, lane 3). These results point to the fact that HAdV protein V is modified with SUMO proteins not only at one but also at different SCMs and that, even further, nSCMs must be involved.

Reduced protein V SUMO conjugation alters the subcellular distribution of the viral protein. To elucidate whether SUMO conjugation with protein V changes its localization in distinct fractions within the nucleus, we analyzed immunofluorescence of the wt protein and the SCM mutants in 6His-SUMO2 HeLa cells (Fig. 4). A stable expression of SUMO2 was chosen to emphasize the difference between wt protein V

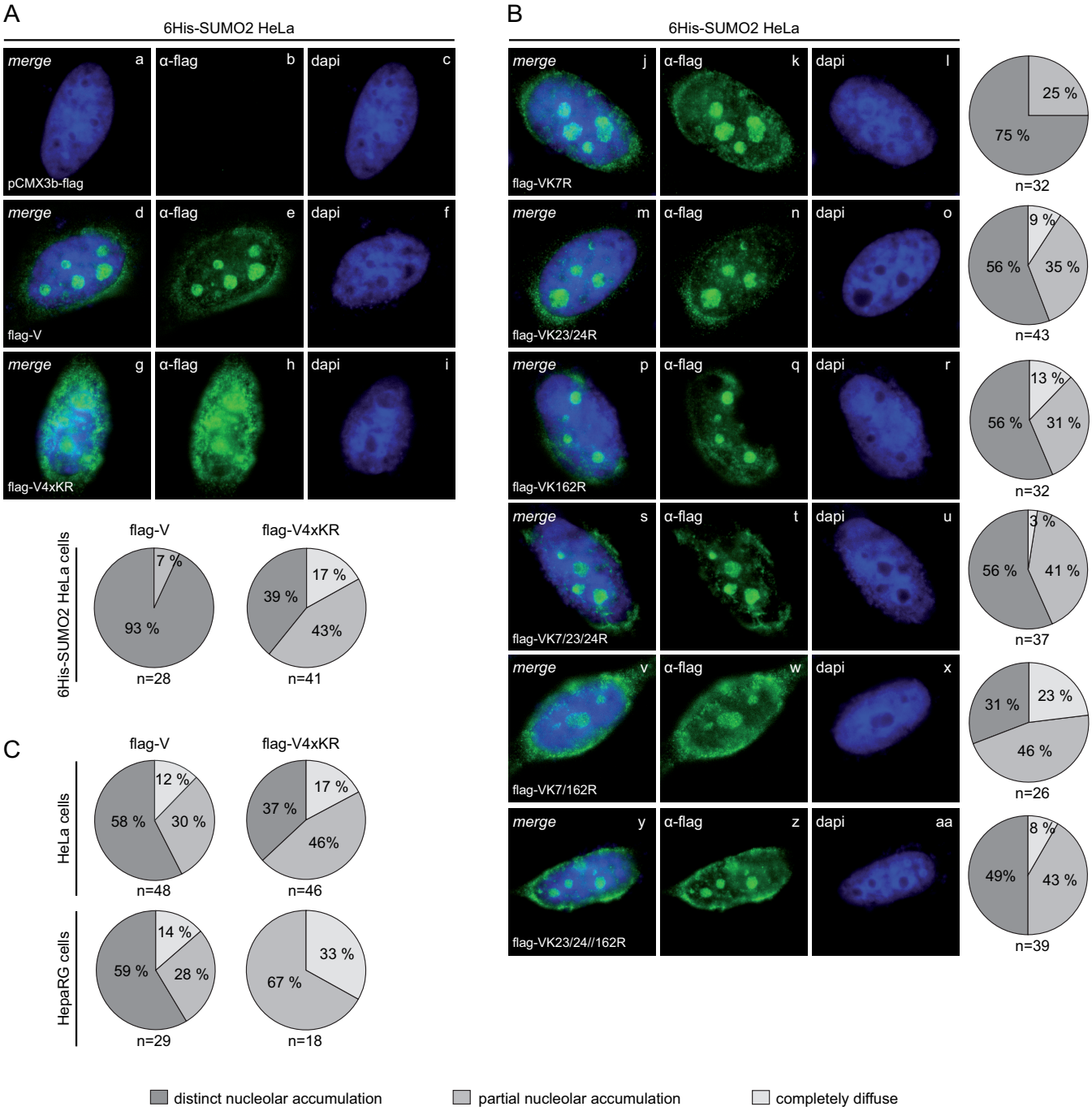

FIG 4 Protein V SUMOylation modulates intracellular distribution of the viral factor. (A and B) 6His-SUMO2 HeLa cells were transfected with 2 μg of a pCMX3b-Flag-V expression plasmid, the different Flag-V SCM mutants, or the empty vector control and fixed with MeOH at 48 h p.t. The cells were stained with pAb anti-V, which was detected with an Alexa 488-conjugated (green) secondary antibody, while nuclei were stained with DAPI (blue). Merged images show the overlay of single images in each row. Images were captured with a Leica fluorescence wide-field microscope. A statistical summary of the captured phenotypes (*n*) is shown (A) in comparison to HeLa and HepaRG cells (C) or on the right (B).

and its SCM mutants. As expected, the most abundant phenotype of Flag-V shows clear accumulations in the nucleus and a weak diffuse signal in the nucleoplasm (Fig. 4A, frames d and e and pie charts). A similar distribution was observed for the single SCM mutant Flag-VK7R (Fig. 4B, frames j and k). In the case of Flag-VK23/24R, Flag-VK162R, Flag-VK7/23/24R, and Flag-VK23/24/162R, the percentage of diffuse protein signal increased (Fig. 4B, frames m to t, y, and z), whereas Flag-V4×KR-transfected cells show distinct nucleolar accumulations only with a maximum of 40% (Fig. 4A, frames g and h

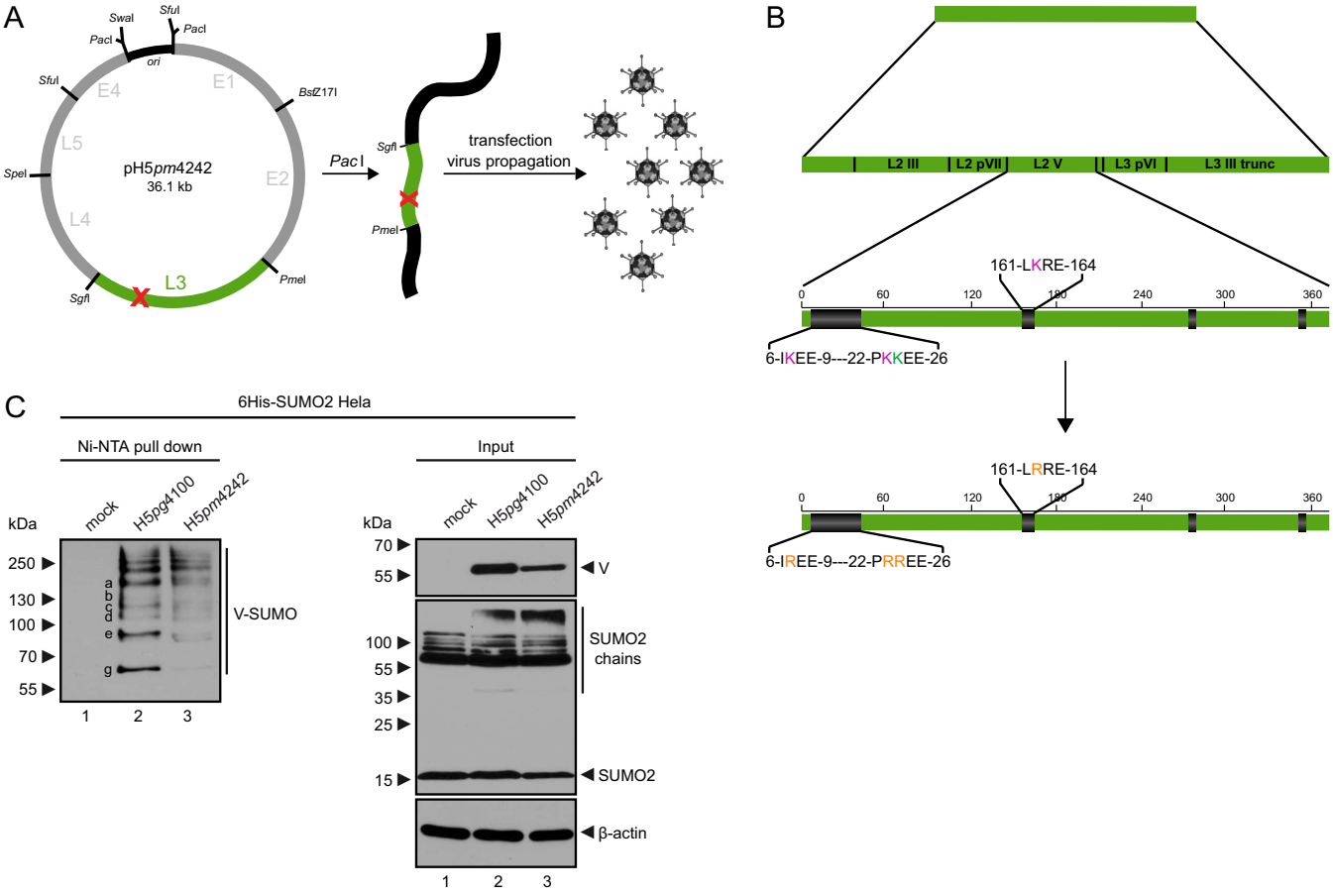

FIG 5 Generation of replication-competent protein V SUMO mutant viruses. (A) A bacmid containing the whole genome of HAdV (pH5*pg*4100) was divided into seven parts by restriction enzymes that cut only one unique site of the viral genome. The resulting fragments of the viral genome were subcloned into vector plasmids that allow the introduction of point mutations or other alterations by site-directed mutagenesis using quick change PCRs. The modified fragment of viral DNA can be cloned back into the viral genome. The newly derived bacmid DNA can be multiplied in bacteria and linearized with the restriction enzyme PacI, which deletes the nonviral part. The linearized, double-stranded viral genome is transfected into human cells to produce infectious particles of the desired virus mutant. (B) HAdV-C5 protein V is part of genome fragment L3, into which we introduced single-nucleotide exchanges in the protein V coding sequence, leading to K → R exchanges within the three SCMs and one neighboring nSCM of the protein. (C) HeLa cells stably expressing 6His-SUMO2 were infected with HAdV wt (H5*pg*4100; MOI of 5) or the HAdV protein V SCM mutant (H5*pm*4242; MOI of 5). The cells were harvested at 24 h p.i. and subjected to a guanidinium chloride buffer. 6His-SUMO conjugates purified by Ni-NTA pulldown, plus control input of total-cell lysate, was resolved by SDS-PAGE and visualized by immunoblotting. Ni-NTA-purified and input proteins were detected using pAb anti-V, MAb anti-6His, and MAb AC-15 (anti-*β*-actin). Molecular masses in kilodaltons are indicated on the left, while corresponding proteins are labeled on the right. Mock means uninfected control.

and pie charts). Although the accumulations remain visible in the majority of transfected cells, they are often blurry and merge with the diffuse fraction of protein V in the nucleoplasm. This type of subcellular distribution was also detected in the majority of 6His-SUMO2 HeLa cells positive for Flag-VK7/162R (Fig. 4A and B, frames v to w). The amount of cells showing distinct protein V accumulations at the nucleoli depends on the cell line and ranges from approximately 60 to 90% (Fig. 4C). Overall, these findings indicate that the lack of certain SCMs within protein V leads to reduced accumulation of the protein at the host nucleoli. A significant effect, however, cannot be assigned to specific lysine residues but depends on the combined absence of at least all three SCMs within protein V.

Protein V SCMs affect virus gene expression and replication. To elucidate the role of this protein V SUMOylation during the course of adenoviral infection, a mutant virus was generated wherein the lysine residues K7, K23, and K162 of the SCM as well as K24, which is part of a neighboring nSCM, are replaced by arginine (R) residues, as before in the construction of the mutant Flag-V4×KR (Fig. 5A and B). We investigated the SUMOylation of protein V during wt (H5*pg*4100) and mutant virus (H5*pm*4242) infection assays in 6His-SUMO2-expressing HeLa cells (Fig. 5C). Total cell lysates were

subsequently purified at 24 h postinfection (p.i.) with a Ni-NTA matrix to pull down 6His-SUMO2 conjugates. Pulldown of protein V from mutant virus-infected cells shows a SUMO2 ladder with severely reduced signal intensities compared to those of protein V from wt-infected cells (Fig. 5C, left panel, lanes 2 and 3). As observed in the transient-transfection experiments (Fig. 3), protein V SUMO bands a, c, e, and f are severely reduced in protein V SCM mutant virus-infected cells, whereas bands b and d are already very weak in wt-infected cells (Fig. 5C, left panel, lanes 2 and 3).

To validate viral replication, we monitored adenoviral progeny production in protein V SCM mutant virus-infected HepaRG cells compared to wt particle synthesis (Fig. 6A). An average of three independent experiments showed approximately a 2.5-fold increase in viral progeny produced at 24 h p.i. in mutant virus-infected cells (Fig. 6A). This increase in viral progeny over HAdV wt particles declines within 72 h p.i., but the ratio remains greater than 1.

The tendency of the mutant virus to produce more infectious particles was also reflected by the equilibrium concentrations of different adenoviral proteins, assessed in an additional time course experiment (Fig. 6B). Early adenoviral proteins E1A, E1B-19K, and E1B-55K appeared 8 h earlier during protein V SCM mutant virus infection than in HAdV infection with wt cells (Fig. 6B, lanes 2 to 4 and 7 to 9). The gene products E2A and E4orf6 were present in higher concentrations at corresponding time points (Fig. 6B, lanes 3, 4, 8, and 9). Similarly, the late protein L4-100K occurred earlier in cells infected with the protein V SCM mutant virus (Fig. 6B, lanes 4 and 8), and many of the capsid proteins showed a stronger signal than that in wt-infected cells (Fig. 6B, lanes 5, 6, and 9 to 11). Only the mutated protein V is less abundant during HAdV protein V SCM mutant infection (Fig. 6B, lanes 5, 6, 10, and 11). Furthermore, levels of the cellular tumor suppressor p53 decrease more efficiently during mutant virus infection (Fig. 6B, lanes 4 to 6 and 9 to 11). In conclusion, the HAdV protein V SCM mutant replication cycle is accelerated in comparison to that of wt virus.

To monitor viral transcription, cells were infected with either HAdV wt or the protein V SCM mutant virus and harvested at 6, 12, or 24 h p.i. Total RNA was isolated, and mRNAs were reverse transcribed. The resulting cDNA was amplified by real-time PCR (RT-PCR) with primer pairs matching different regions of the adenoviral genome to reveal the relationship between early and late mRNAs in the differently infected HepaRG cells. As with the previous time course experiments at the protein level, all viral mRNAs investigated were synthesized earlier or with enhanced concentrations at particular time points in protein V SCM mutant virus-infected cells (Fig. 6C). Interestingly, E1A mRNA concentrations were already ~2-fold higher at the early time points of 6 and 12 h p.i. This observation was similar for the early viral mRNAs encoding E1B-55K and E4orf6, albeit they were detected in protein V SCM mutant virus-infected cells only at the earliest time point measured, 6 h p.i. (data not shown). The elevated mRNA concentrations of E2A were even more pronounced. Already at 6 h p.i. an approximately 12.5-fold excess of E2A-mRNA could be detected, which declined later on, as also found for the other viral mRNAs (Fig. 6C).

Comparable to adenoviral protein analysis, late viral mRNAs were also influenced (Fig. 6C). Interestingly, not only hexon mRNA but also protein V mRNA occurred already at 12 h after protein V SCM mutant virus infection, whereas these mRNAs cannot be detected earlier than 24 h after HAdV wt infection. However, the protein V SCM mutant was the only protein with reduced steady-state concentrations in the protein time course experiment (Fig. 6B). Taken together, these results further underline an enhanced efficacy of the HAdV protein V SCM mutant virus early during infection, which occurs prior to translation of adenoviral proteins.

To substantiate our data, we repeated virus yield (Fig. 6D) and protein synthesis (Fig. 6E) analyses in another human cell line. Our data showed that also in H1299 cells adenoviral progeny production in protein V SCM mutant virus-infected cells was more efficient than that after wt infection (Fig. 6D). In accordance with the results obtained in HepaRG cells, the mutant virus produces enhanced levels of early viral proteins, as assessed in an additional time course experiment (Fig. 6E).

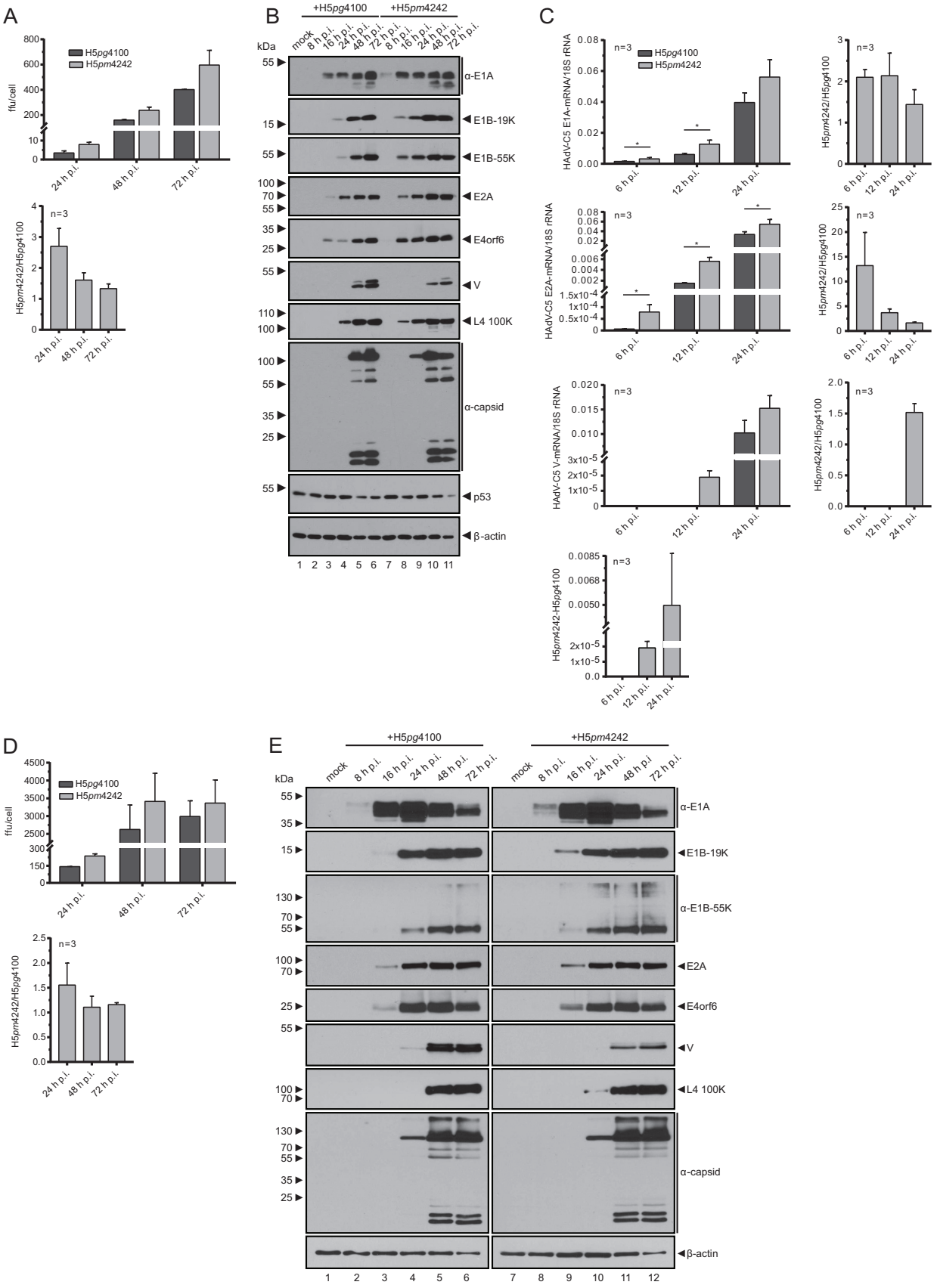

FIG 6 Role of protein V SUMOylation during productive infection. HepaRG cells (A) or H1299 cells (D) were infected with HAdV wt (H5*pg*4100; MOI of 20) or protein V SCM mutant virus (H5*pm*4242; MOI of 20) and harvested at 24, 48, or 72 h p.i. Viral progeny were isolated and titrated by

(Continued on next page)

Protein V SUMOylation promotes nucleolus association of the viral factor. To reveal the effect of protein V mutations on subcellular protein distribution during productive infection, cells infected with HAdV wt or the protein V SCM mutant virus were prepared for immunofluorescence analysis at 24 h p.i. The cells were doubly stained for protein V and either E1A (Fig. 7A), E1B-55K (Fig. 7B), or E2A (Fig. 7C), regulatory adenoviral proteins showing higher concentrations at early time points during protein V SCM mutant virus infection (Fig. 6B). E1A was diffusely distributed throughout the whole nucleus of infected cells except the nucleoli (Fig. 7A, frames g and k). E1B-55K accumulated in speckled fractions of different sizes and shapes within the cytoplasm and showed an additional diffuse signal in the nucleus (Fig. 7B, frames g and k). Consequently, none of the two proteins showed noticeable colocalization with protein V at the nucleoli. Only parts of their diffuse fractions overlap diffuse portions of protein V (Fig. 7A and B, frames e and i). E2A forms spherical structures within the nucleus known to be the sites of viral replication. They varied from small filled dots to huge hollow spheres in both cells infected with HAdV wt and the protein V SCM mutant virus (Fig. 7C, frames g and k). Hence, no difference in the localizations of essential early viral proteins can be detected between HAdV wt- and protein V SCM mutant virus-infected HepaRG cells.

Furthermore, the sites of viral replication and the host nucleoli where protein V accumulates exclude each other. This leads to separate fractions of protein V and E2A during wild-type infection, apart from the diffuse portion of protein V (Fig. 7C, frame e) (11). This finding was confirmed in a colocalization study of frames f and g where the thresholded Mander's split coefficients resulted in a tM1 of 0.24 for the red channel (protein V) and a tM2 of 0.54 for the green channel (E2A). This phenomenon was less pronounced in 42% of protein V SCM mutant virus-infected HepaRG cells ($n = 12$) where some portion of protein V accumulated in small dots at the periphery of the nucleus, close to the nuclear membrane (Fig. 7C, frame j). According to the intensity overlay of red and green channels in the nuclear area, these spherical structures indeed colocalized with corresponding dots of E2A, leading to a gray signal (Fig. 7C, right panel, bottom). In contrast, the green intensity corresponding to E2A clearly dominates the red signal in wild-type-infected cell nuclei (Fig. 7C, right panel, top). In protein V SCM mutant virus-infected cells, E2A signal intensities colocalize with those of protein V (tM2 of 0.85), and a greater nuclear portion of protein V correlates with E2A signals (tM1 of 0.48) than in wild-type-infected cells (tM1 of 0.24).

In addition, V4×KR accumulated less clearly within the nucleus than wt protein V (Fig. 7A to D). An average of four independent immunofluorescence analyses in which protein V was stained yielded 73% of HAdV wt-infected cells showing clear accumulations of protein V at host nucleoli. In contrast, this phenotype was seen in only 42% of HepaRG cells infected with the protein V SCM mutant virus (Fig. 7E). This tendency of the protein V SCM mutant to be more diffusely distributed in the host nucleus was also seen in each individual experiment although the experimental conditions differed slightly (Fig. 7D). In conclusion, the lack of SCMs within HAdV protein V reduces the ability of the protein to accumulate at the host nucleoli.

FIG 6 Legend (Continued)

visualizing the infected cells via immunofluorescence to determine the yield. The averages of $n = 3$ independent experiments, each done in triplicate, were plotted on bar graphs to emphasize the ratio of the protein V SCM mutant virus to HAdV wt (H5*pm*4242/H5*pg*4100) at each time point investigated. Error bars indicate the standard deviation. FFU, fluorescence-forming units. (B and E) HepaRG cells (B) or H1299 cells (E) were infected with HAdV wt (H5*pg*4100; MOI of 20) or protein V SCM mutant virus (H5*pm*4242; MOI of 20) and harvested at 8, 16, 24, 48, or 72 h p.i. Total cell lysates were resolved by SDS-PAGE and visualized by immunoblotting. Proteins were detected using MAb M73 (anti-E1A), pAb anti-19K, MAb 2A6 (anti-E1B-55K), MAb B6-8 (anti-E2A), MAb RSA3 (anti-E4orf6), MAb 6B10 (anti-L4-100K), pAb anti-V, pAb L133 (anti-capsid), MAb DO-1 (anti-p53), and MAb AC-15 (anti-β-actin). Molecular masses in kilodaltons are indicated on the left, while corresponding proteins are labeled on the right. Mock, uninfected control. (C) HepaRG cells were infected with HAdV wt (H5*pg*4100; MOI of 20) or protein V SCM mutant virus (H5*pm*4242; MOI of 20) and harvested at 6, 12, or 24 h p.i. Total RNA was isolated from the cells, mRNA was reverse transcribed, and the resulting cDNA was amplified by RT-PCR with primer pairs specific for a certain viral sequence and primer pairs against a coding sequence (CDS) fragment of cellular 18S rRNA (Table 1). HAdV mRNA amounts are depicted relative to the amounts of cellular 18S rRNA as an average of $n = 3$ independent experiments. Error bars indicate the standard deviations. RT-PCR was performed in technical duplicates for each experiment, and the statistics were calculated with a two-tailed, unpaired *t* test for each time point. *, $P < 0.05$. At the bottom, the ratio of the amount of the protein V SCM mutant virus to that of the HAdV wt (H5*pm*4242/H5*pg*4100) is illustrated for each time point investigated.

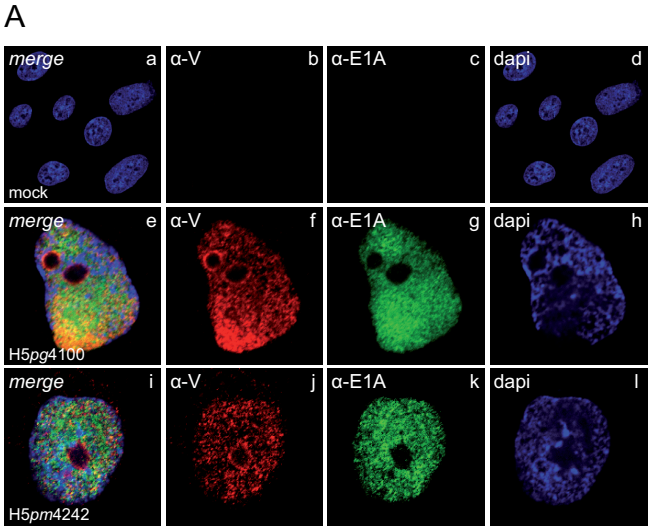

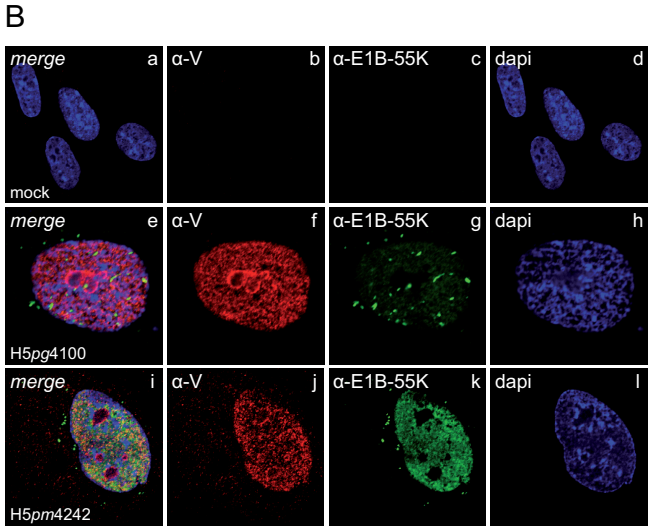

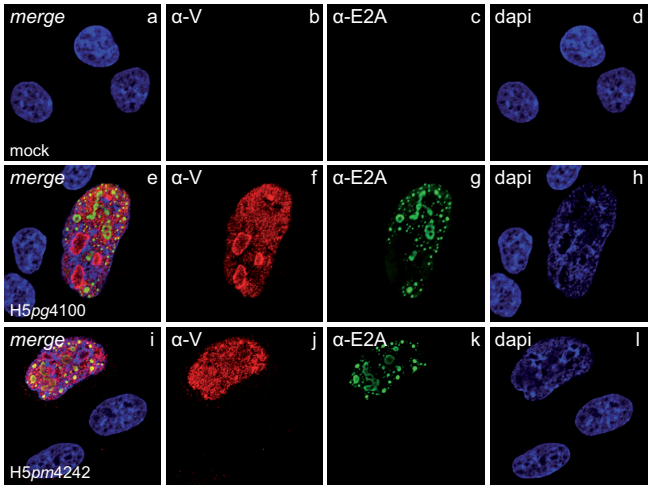

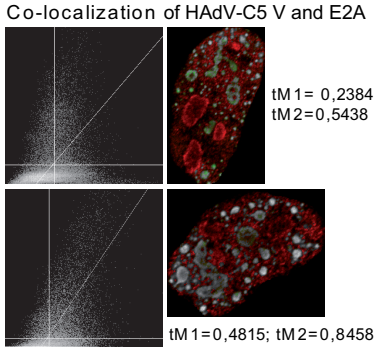

D

experimental condition	1	2	3	4
Alexa488-conjugated sec. ab			x	x
Cy3-conjugated sec. ab	x	x		
confocal fluorescence microscope	x		x	
wide field fluorescence microscope		x		x
24 h p.i.	x			x
32 h p.i.		x	x	
PFA-fixation	x	x	x	
MeOH-fixation				x

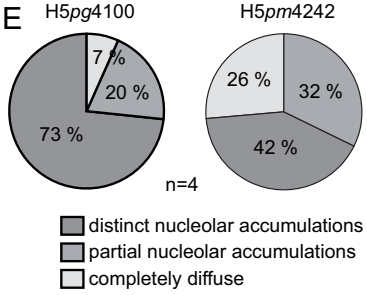

FIG 7 SUMO conjugation promotes protein V nucleolus association. HepaRG cells were infected with the HAdV wt (H5*pg*4100; MOI of 20) or HAdV protein V SCM mutant (H5*pm*4242; MOI of 20) and fixed with 4% PFA at 24 h p.i. To visualize protein V, the cells were treated with pAb anti-V. E1A was visualized with MAb M73 (anti-E1A) (A), E1B-55K was visualized with MAb 2A6 (anti-E1B-55K) (B), and E2A was visualized with MAb B6-8 (anti-E2A) (C). Primary antibodies were detected with secondary antibodies conjugated to Alexa 488 (green) or Cy3 (red), and nuclei were stained with DAPI (blue). Merged images show the overlay of single images of each row, and mock refers to the uninfected control. Images were captured with a Nikon confocal microscope. To the right of panel C, the colocalization of HAdV protein V and E2A is depicted by two-dimensional histograms, which correlate the pixel intensities of two channels (left) and the corresponding channel overlay of the analyzed regions of interest (right); tM is the thresholded Mander's split coefficient where number 1 corresponds to the red channel (protein V) and number 2 corresponds to the green channel (E2A). (D) The experimental conditions for individual experiments 1 to 4. Examples from experimental condition 1 are shown in panels A to C. (E) Statistical summary of captured phenotypes in $n = 4$ independent experiments.

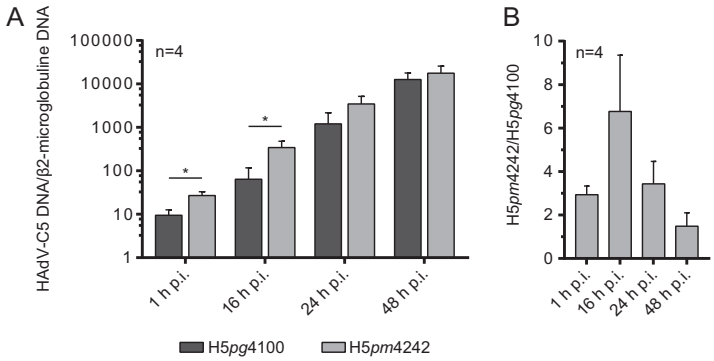

FIG 8 Reducing protein V SUMOylation promotes viral DNA synthesis. HepaRG cells were infected with the HAdV wt (H5*pg*4100; MOI of 20) or protein V SCM mutant virus (H5*pm*4242; MOI of 20) and harvested at 1, 16, 24, or 48 h p.i. Genomic DNA was isolated from the cells and amplified by RT-PCR with primer pairs specific for an HAdV-C5 hexon coding sequence fragment or specific for a fragment of the cellular single-copy gene β2-microglobulin (Table 1). (A) HAdV DNA amounts are depicted relative to the amounts of the cellular single-copy gene as an average from $n = 4$ independent experiments. Error bars indicate standard deviations. RT-PCR was performed in technical duplicates for each experiment, and statistics were calculated with a two-tailed, unpaired *t* test. *, $P < 0.05$. (B) Ratio of the protein V SCM mutant virus and HAdV wt DNAs (H5*pm*4242/H5*pg*4100) at each time point investigated.

Reduction of protein V SUMOylation promotes viral DNA replication. As a consequence of earlier viral protein expression during HAdV protein V SCM mutant virus infection than in wt infection, it was expected that the onset of viral DNA replication might be accelerated as well. To test this hypothesis, HepaRG cells were infected with either the protein V SCM mutant or the wt virus and harvested at 1, 16, 24, and 48 h p.i. The genomic DNA of collected samples was isolated, purified, and analyzed by PCR. At each time point, the HAdV DNA amount was determined relative to that of the one-copy gene β2-microglobulin to avoid false differences due to the various DNA contents of the samples. This approach indeed confirmed accelerated viral DNA replication during protein V SCM mutant virus infection (Fig. 8), showing its greatest advantage at 16 h p.i. (Fig. 8B), shortly after the onset of viral DNA replication. This difference decreases as infection proceeds and levels out 2 days after infection (Fig. 8). Interestingly, already at 1 h p.i. more viral DNA was isolated from mutant virus-infected HepaRG cells than from those infected with wt HAdV in four independent experiments, indicating some additional effect on virus entry processes (Fig. 8).

DISCUSSION

Here, we report that disrupting protein V consensus SUMO conjugation motifs (SCMs) by site-directed mutagenesis results in a global acceleration of viral replication and progeny production. Mutation of the three SCMs within HAdV protein V causes a loss of distinct SUMO signals and an overall reduction in the intensities of the remaining ones. This significant reduction of protein V SUMOylation during mutant virus infection could be partially caused by smaller amounts of the protein than in HAdV wt infection. However, the loss of signal intensity is more pronounced for certain SUMO signals, which could refer to mono-or polyubiquitinylation. The lack of protein V SCM reduced SUMOylation of the protein during transient-transfection studies as well as during HAdV infection. Hence, the loss of certain SUMO signals is apparently the actual cause of the observed accelerated viral life cycle. This would be an interesting phenotype since it matches the emerging hypothesis of SUMOylation-dependent regulation of proteins involved in intrinsic and innate immunity (15). However, this raises the question of why the virus would evolve SUMO conjugation sites in protein V if this is detrimental for efficient infection. Our observations suggest that it might represent a bottleneck for enhancement of virus replication, as adenoviruses need to not kill the host before spread of the infection.

PML bodies represent SUMOylation hot spots of the cell. The interplay of viruses

with infected host cells is influenced by SUMOylation of both viral and cellular proteins (16, 17). Hence, the SUMOylation of proteins has emerged as one key posttranslational modification (PTM). SUMO proteins, which belong to the family of ubiquitin-like (UBL) modifiers, can be covalently bound to target proteins or noncovalently interact with SIMs of other proteins to affect their function. It is widely assumed that PML nuclear bodies are needed to concentrate proteins in a defined area to increase reaction efficiencies and facilitate their regulation. Here, we observed that there are different protein V fractions in the infected host cell nucleus. Next to the known localization of protein V at host nucleoli, we find a large protein V portion distributed over the whole nucleoplasm and also a partial colocalization of HAdV protein V with PML. However, these aggregates no longer have their typical sizes and shapes. They appear larger and often localize in proximity to the nuclear envelope. We were unable to detect protein V interaction with any constituent PML-NB factor, i.e., PML, Sp100, or Daxx. However, since the composition of PML-NBs is dynamic, a temporary interaction with specific host determinants of the PML-NBs remains possible.

Interestingly, the equilibrium of early viral protein concentrations was already elevated during infection with the HAdV protein V SCM mutant (H5*pm*4242). However, newly translated protein V, lacking its SCM, cannot be the cause of this phenotype since this protein is expressed only in the late phase of adenoviral infection. This points to incoming modified protein V having an influence on early viral protein levels. In accordance with this hypothesis, adenoviral mRNA concentrations are also already influenced at a time point when viral transcription has just started and when only incoming virion proteins of HAdV can be present. This is especially striking in the case of E1A mRNA since E1A is known to be the first adenoviral protein expressed. Whether viral transcription is influenced directly or whether the viral mRNAs might, rather, be stabilized posttranscriptionally remains to be clarified in future experiments.

So far, protein V has not been identified as an RNA-binding protein (RBP). Moreover, alignment of its primary structure with known RNA recognition motifs (RRM), zinc fingers, or the KH domain (18) identified no matches (https://blast.ncbi.nlm.nih.gov/Blast.cgi?PROGRAM=blastp&PAGE_TYPE=BlastSearch&LINK_LOC=blasthome) although protein V could act on RNA in a complex with other cellular or even viral RBPs.

Another explanation for the accelerated protein V SCM mutant virus phenotype could relate to viral entry and nuclear uptake of the viral core. This possibility was supported by monitoring viral DNA replication since already at 1 h p.i. more viral DNA could be detected in protein V SCM mutant virus-infected cells.

Immunoblotting of proteins originating from three different infected cell lines revealed that protein V SCM occurs in lower steady-state concentrations than wt protein V. However, protein V mRNA expression is accelerated during protein V SCM mutant virus infection, just as with all the adenoviral mRNAs investigated. Some reasons for lower mutant protein V levels could be lower protein stability, relocalization of protein V SCM to insoluble fractions such as the nuclear matrix, or even degradation of the protein. However, the last possibility seems unlikely since the protein V concentration increased over time.

SUMO conjugation to a protein is linked to increased protein stability because competitive ubiquitinylation is prevented at the corresponding lysine residue and because polyubiquitination represents a signal for proteasomal degradation. However, protein V SCM stability would not be affected by increasing ubiquitinylation since the corresponding lysine residues were replaced by arginines. However, these amino acid substitutions at four individual positions in protein V could affect the protein conformation and thereby its stability, function, or both. To minimize the probability of such unwanted side effects, arginine was specifically chosen as a substitute for lysine since arginine retains the local and net charge of the altered protein. In addition, the effect of these point mutations on structural elements of HAdV protein V was evaluated by I-TASSER (Iterative Threading ASSEmbly Refinement). Since no change in any secondary structure element was seen and since the accuracy of tertiary structure predictions was

low (data not shown), the probability of structural changes within protein V was assessed as low.

Notably, HAdV protein V has been predicted to be a protein of low structural order by different algorithms, including APSSP, version 2 (Advanced Protein Secondary Structure Prediction Server), PSIPRED, version 3.3, and I-TASSER. Intrinsically disordered proteins (IDPs) often contain a combination of intrinsically disordered regions (IDRs) and structured domains, as was predicted for HAdV protein V. The high degree of disorder results in high protein flexibility, allowing for dynamic switching between conformations. This allows IDPs to interact with a variety of different target molecules, such as DNA, other proteins, complexes, or PTMs. Upon binding to different targets, many IDPs form well-defined induced-fit structures that depend on the binding partner (19, 20). For instance, binding of HAdV protein V to DNA in solution was shown to be sequence independent, mainly depending on the soluble N terminus of the protein (aa 1 to 200) (3, 6, 21). However, inside adenoviral virions fewer regions of protein V contact the viral genome, indicating that DNA binding regions are masked sterically or through interactions with other viral proteins, and this results in a higher-order complex that is destabilized during capsid disassembly (6).

Possibly, HAdV protein V, lacking its SCM, could change its behavior within mature adenoviral particles and thereby affect their stability. A preweakening of adenoviral virions might facilitate viral uptake and disassembly, which starts already at the cell surface (22). If the presence of less protein V is the cause of reduced protein V signals after immunoblotting of protein V SCM mutant virus-infected cells, then a lack of protein V incorporation into new infectious particles would also be imaginable. Only a few studies investigating posttranslational modifications within viral particles have been published so far. A very early one in the 1980s revealed the presence of phosphorylated, adenoviral proteins. Indeed, phosphorylated protein IIIa could be found in mature particles, whereas protein V phosphorylation disappeared during virion maturation (23). However, other PTMs of adenoviral proteins within viral particles have never been reported. Very recently, it could be shown that the major core protein VII is acetylated at specific sites but only in cell extracts and not within purified viruses (24). The possibility remains that a change in protein V SUMOylation already influences the stability within adenoviral virions and facilitates their uptake into host cells.

The hypothesis of adenoviral protein V being a strictly regulated protein fits the finding that protein V is necessary for viral progeny production. An HAdV mutant virus, depleted of protein V, could be rescued only through the coding region of protein μ acquiring three additional point mutations. Otherwise, the production of infectious progeny failed (25). In addition, there is evidence that nucleoplasmic nucleophosmin (B23.1, or NPM1) is required for efficient adenoviral replication (26, 27). NPM1 is a nucleolar phosphoprotein, which is only modestly expressed in human primary cells. In contrast, it is overexpressed in various types of human tumors (28) where it is localized in the nucleoli as well as in the nucleoplasm (29).

The SCM mutation within the coding sequence of HAdV protein V leads to a decrease of the overall protein signal after immunoblotting as well as in immunofluorescence analysis of infected cells compared to levels in cells infected with HAdV wild type. However, not only the amounts of detected protein V differ between viral infections but also protein V, lacking its SCM, seems to have a reduced affinity to accumulate at host nucleoli. Transfection experiments further revealed that the mutation of a single SCM within HAdV protein V does not have a significant impact on the localization of the protein in different cell lines. Only if all three SCMs are altered are protein V accumulations significantly less pronounced. This indicates that the SUMOylated protein V is preferentially directed to nucleoli.

In conclusion, our findings show that protein V SUMO modification negatively regulates the HAdV life cycle and might represent a novel antiviral target structure for therapy approaches. Conversely, blocking SUMO conjugation to HAdV protein V protein could potentially impact gene vector development and efficacy during production.

TABLE 1 Primers used in this study

Primer description	Primer sequence
18S rRNA	5′-CGGCTACCACATCCAAGGAA-3′ 5′-GCTGGAATTACCGCGGCT-3′
Flag-V	5′-ACAGGATCCTCCAAGCGCAAAATCAAAGAAGAGATGC-3′ 5′-ACAGAATTCTTAAACGATGCTGGGGTGGTAGCG-3′
Flag-VK7R	5′-CCAAGCGCAAAATCAGAGAAGAGATGCTCC-3′ 5′-GGAGCATCTCTTCTCTGATTTTGCGCTTGG-3′
Flag-VK23/24R	5′-CTATGGCCCCCCGAGGAGGGAAGAGCAGGATTAC-3′ 5′-GTAATCCTGCTCTTCCCTCCTCGGGGGGCCATAG-3′
Flag-VK162R	5′-CCAAGCGCAAAATCAGAGAAGAGATGCTCC-3′ 5′-CACCAGACTCGCGCCTTAGGCCGCGCTTTT-3′
E1A	5′-GTGCCCCATTAAACCAGTTG-3′ 5′-GGCGTTTACAGCTCAAGTCC-3′
E2A	5′-GAAATTACGGTGATGAACCCG-3′ 5′-CAGCCTCCATGCCCTTCTCC-3′
Protein V	5′-CCCGAAAGCTAAAGCGGGTC-3′ 5′-CGTAAAGACTACGGTGGTGC-3′
Hexon	5′-CGCTGGACATGACTTTTGAG-3′ 5′-GAACGGTGTGCGCAGGTA-3′
β2-Microglobulin	5′-TGAGTATGCCTGCCGTGTGA-3′ 5′-CCATGTGACTTTGTCACAGCCCAAGATAGTT-3′

MATERIALS AND METHODS

Cell lines and culture conditions. H1299 (no. CRL-5803; ATCC Global Bioresource Center) and HeLa cells, 6His-SUMO1 HeLa cells, or 6His-SUMO2 HeLa cells (kind gift from Ron T. Hay, University of Dundee, Scotland) stably expressing 6His-SUMO1 or 6His-SUMO2 (30) were grown in Dulbecco's modified Eagle's medium supplemented with 5% fetal calf serum, 100 U/ml penicillin, and 100 μg/ml streptomycin in a 5% CO_2 atmosphere at 37°C. For HepaRG cells, the medium was supplemented with 10% fetal calf serum, 100 U/ml penicillin, 100 μg/ml streptomycin, 5 μg/ml of bovine insulin, and 0.5 μM hydrocortisone. 6His-SUMO HeLa cell lines were maintained under 2 μM puromycin selection. All cell lines were frequently tested for mycoplasma contamination.

Plasmids and transient transfections. HA-V proteins were expressed from their respective cDNAs under the control of the cytomegalovirus (CMV) immediate early promoter from pcDNA3 (Invitrogen)-based vector plasmids. Flag-V proteins examined in this study were expressed from their respective cDNAs under the control of the CMV immediate early promoter from the pCMX3b vector plasmid. The expression plasmids were generated with the oligonucleotide primers indicated in Table 1. Flag-V mutants were derived through single-nucleotide exchanges by site-directed mutagenesis using the oligonucleotides shown in Table 1. For transient transfections, subconfluent cells were treated with a mixture of DNA and linear polyethylenimine (PEI; 25 kDa) as described before (31).

Viruses. H5*pg*4100, which contains deletions in the E3-coding region, served as the wild-type (wt) HAdV-C5 virus (32). H5*pm*4242 carries four point mutations within the protein V coding sequence. It was derived by site-directed mutagenesis (32) using the oligonucleotide primers indicated in Table 1.

All viruses were propagated and titrated in H1299 cells. For this, infected cells were harvested at 3 to 5 days p.i. and lysed by three freeze-thaw cycles. The supernatant containing HAdV was used to reinfect subconfluent H1299 cells. At 24 h p.i. the concentration of infectious particles was determined by immunofluorescence staining of the adenoviral DNA binding protein E2A/DBP as described before and is represented as the number of fluorescence-forming units/cell (33). HAdV cells were supplemented with 10% (vol/vol) sterile glycerol to be preserved at −80°C. At 4°C, viral titers remain constant for several weeks.

Adenoviral progeny of infected cells was determined at 24 h, 48 h, and 72 h p.i. Cells harvested at these time points were stored at −20°C until samples were complete. Viral particles were released through repeated freeze-thaw cycles, and subconfluent H1299 cells were reinfected with dilutions of the supernatants ranging from 10^{-2} to 10^{-4}. Viral titers were determined as described before and are represented as the number of fluorescence-forming units/cell (34).

Antibodies and protein analysis. Primary antibodies specific for viral proteins included E1B-55K mouse monoclonal antibody (MAb) 2A6 (35), E4orf6 mouse MAb RSA3 (36), L4-100K rat MAb 6B-10 (37), E2A-72K mouse MAb B6-8 (38), E1A mouse MAb M73 (39), E1B-19K rabbit polyclonal antibody (pAb) (40), HAdV-C5 rabbit polyclonal serum L133 (41), and protein V rabbit pAb (kindly provided by D. A. Matthews,

University of Bristol, United Kingdom). Primary antibodies specific for cellular and ectopically expressed proteins included anti-Flag mouse MAb M2 (Sigma-Aldrich, Inc.), anti-HA tag rat MAb 3F10 (Roche), anti-His tag mouse MAb (Clontech), anti-p53 mouse MAb Do-1 (Santa Cruz), anti-B23 mouse MAb FC-61991 (Invitrogen), and β-actin mouse MAb AC-15 (Sigma-Aldrich, Inc.). Secondary antibodies conjugated to horseradish peroxidase (HRP) for detection of proteins by immunoblotting were anti-rabbit IgG, anti-mouse IgG, anti-rat IgG (Jackson/Dianova).

Protein extracts were prepared in radioimmunoprecipitation assay (RIPA) lysis buffer (12) on ice for 30 min. Total cell lysates were sonicated for 30 s (40 pulses; output, 0.6 and 0.8 impulses/s) before the cell debris was removed (11,000 rpm, 3 min, 4°C). Protein concentration was determined photometrically with Bradford reagent (Bio-Rad). For Ni-NTA pulldown, cells were harvested 48 h after treatment. Twenty percent of total cells was pelleted to determine steady-state protein concentrations as described above, whereas the remaining cells were resuspended in 5 ml of guanidinium hydrochloride (GuHCl) lysis buffer (0.1 M Na_2HPO_4, 0.1 M NaH_2PO_4, 10 mM Tris-HCl, pH 8.0, 20 mM imidazole, and 5 mM β-mercaptoethanol). Lysed cells in GuHCl buffer were sonicated for 30 s (40 pulses; output 0.6 and 0.8 impulses/s) and supplemented with 25 μl of Ni-NTA agarose (Qiagen) prewashed with GuHCl. The samples were incubated overnight at 4°C, followed by centrifugation (4,000 rpm, 10 min, 4°C). Sedimented agarose was washed once with buffer A (8 M urea, 0.1 M Na_2HPO_4, 0.1 M NaH_2PO_4, 10 mM Tris-HCl, pH 8.0, 20 mM imidazole, and 5 mM β-mercaptoethanol) and two times with buffer B (8 M urea, 0.1 M Na_2HPO_4, 0.1 M NaH_2PO_4, 10 mM Tris-HCl, pH 6.3, 20 mM imidazole, and 5 mM β-mercaptoethanol). 6His-SUMO conjugates were eluted from the Ni-NTA agarose with 30 μl of nickel resin elution buffer (200 mM imidazole, 5% [wt/vol] SDS, 150 mM Tris-HCl [pH 6.7], 30% [vol/vol] glycerol, 720 mM β-mercaptoethanol, 0.01% [wt/vol] bromophenol blue).

All protein samples were separated by SDS-PAGE after denaturation (5× SDS sample buffer, 95°C, 3 min). Proteins were transferred to nitrocellulose blotting membranes (0.45-μm pore size) and visualized by immunoblotting (Western blotting). The protein transfer was performed in a Trans-Blot Electrophoretic Transfer Cell (full wet mode; Bio-Rad) in Towbin buffer (25 mM Tris-HCl [pH 8.3], 200 mM glycine, 0.05% [wt/vol] SDS, 20% [vol/vol] methanol) at 400 mA for 90 min. Membranes were incubated overnight at 4°C in phosphate-buffered saline (PBS) containing 5% nonfat dry milk. They were washed three times in PBS–0.1% Tween 20 (PBST) before they were incubated for 3 h with the appropriate primary antibody in PBST. Membranes were washed again three times in PBST before being incubated for 1 h with a secondary antibody conjugated to HRP (1:10,000 [vol/vol] in PBST) containing 3% nonfat dry milk. After three washes in PBST, the bands were visualized by enhanced chemiluminescence (ECL) as recommended by the manufacturer (Pierce) on X-ray films (CEA RP film). Autoradiograms were scanned and cropped using Adobe Photoshop CS6. Final figures were prepared using Adobe Illustrator CS6 software.

Indirect immunofluorescence. For indirect immunofluorescence, 2×10^5 adherent, eukaryotic cells were seeded on sterile glass coverslips positioned in six-well cell culture dishes. Twenty-four hours later the cells were treated as experimentally required, and at the time point of interest, all treated cells were fixed with either methanol at −20°C (10 min) or paraformaldehyde (PFA; 4% [vol/vol] in PBS) at room temperature (20 min). If fixed with PFA, the cells had to be permeabilized in phosphate-buffered saline (PBS) with 0.5 Triton X-100 for 10 min at room temperature prior to 10 min of blocking in Tris-buffered saline–BG (TBS-BG; BG consists of 5% [wt/vol] bovine serum albumin [BSA] and 5% [wt/vol] glycine). Coverslips were treated for 30 min in a humidity chamber with the primary antibody (indicated in the figure legend) diluted in PBS. Afterwards, the cells were incubated for 20 min with the corresponding secondary antibody diluted in PBS and conjugated to Alexa 488 (Invitrogen), Cy3 (Jackson ImmunoResearch), fluorescein isothiocyanate (FITC; Jackson ImmunoResearch), or Texas Red (Jackson ImmunoResearch). Finally, nuclei were stained with 4,6-diamidino-2-phenylindole (DAPI) in PBS (1:1,000, vol/vol) for 5 min before the cells were mounted in glow medium (Energene). All steps were separated by three washing steps with PBS (5 min each). DAPI was rinsed off with double-distilled water. Digital images were acquired with either a confocal laser scanning microscope (Nikon) using the NIS-Elements software or a wide-field fluorescence microscope (Leica) using the Leica Application Suite. Images were processed with Adobe Photoshop CS6 and assembled with Adobe Illustrator CS6. Colocalization analysis was calculated and visualized with Fiji (colocalization threshold plug-in).

Isolation and quantification of nucleic acids. To isolate RNA, cell samples (4×10^6 cells) in 600 μl of TRIzol (ThermoFisher) were incubated with 60 μl of 1-bromo-3-chloropropane for 10 min at room temperature and centrifuged at 12,000 × *g* for 15 min at 4°C. Contained nucleic acids in the aqueous phase were precipitated with 500 μl of isopropanol (12,000 × *g*, 10 min, 4°C), washed with 1 ml of ethanol (75%, vol/vol) by vortexing, and pelleted (7, 500 × *g*, 5 min, 4°C). The pellets were air dried for 5 to 10 min and resuspended carefully in 80 μl of RDD buffer containing 10 μl of RNase-free DNase I (Qiagen) to digest traces of the remaining DNA for 30 min at room temperature. DNase I was heat inactivated (75°C, 5 min), and RNAs were precipitated with RNase-free LiCl solution (final concentration, 2.5 M; Applied Biosystems) for 30 min at −20°C. RNAs were pelleted at 16, 000 × *g* for 20 min at 4°C and washed with ice-cold ethanol (75%, vol/vol). RNA pellets were air dried for 5 to 10 min and dissolved for 10 min at 58°C in nucleic acid-free water (Promega).

Purified RNA was transcribed into cDNA by use of a reverse transcription system (Promega) according to the manufacturer's protocol. The reaction mixture was primed with oligo(dT) primers to select for mRNAs. Transcribed cDNAs were stored at −20°C. All samples were additionally prepared without the reverse transcriptase to determine the level of background DNA contamination during RT-PCR. No sample showed DNA concentrations higher than random background levels.

To isolate genomic DNA from cultured cells, collected cell pellets were resuspended in 200 μl of PBS (phosphate-buffered saline) and supplemented with 20 μl of proteinase K (Sigma-Aldrich). All further

steps have been performed according to the *QIAamp DNA Mini and Blood Mini Handbook* (42). Purified genomic DNA was dissolved for 5 min in 200 μl of nucleic acid free-water (Promega) per sample and stored at −20°C.

Quantification of cDNA or genomic DNA was realized through real-time quantitative PCR (qPCR). Purified samples were diluted 1:100 with nucleic acid-free water (Promega), and 4.5 μl per sample was mixed with 5 μl of SensiMix Plus SYBR (Quantace) and 0.5 μl of appropriate primer pairs (5 μM primer mix) (Table 1).

All primers amplify a short fragment of 100 to 200 bp within a DNA coding sequence. The reaction was performed in a Rotor-Gene 6000 (Corbett Life Sciences) machine. Each sample was measured in technical duplicates to determine the average threshold cycle (C_T). Levels of viral mRNA were calculated relative to the level of cellular 18S rRNA, whereas genomic viral DNA was calculated relative to amount of the cellular one-copy gene β2-microglobulin. Recording the melting curves as well as agarose gel electrophoreses of the RT-PCR products ensured the purity of samples/products. Obtained data were processed with Rotor-Gene Q, version 2.3.1 (Qiagen), software; calculations were done with Microsoft Excel, and statistical analysis was performed in the form of unpaired, two-tailed *t* tests (GraphPad Prism, version 5). Graphs were generated in Prism, version 5, as well, whereas final figures were generated with Adobe Illustrator CS6.

ACKNOWLEDGMENTS

We greatly appreciate the critical comments from and scientific discussions with Nicole Fischer (University Hospital Hamburg-Eppendorf, Germany) and Ron T. Hay (University of Dundee, Scotland). Moreover, we thank David Matthews (University of Bristol, United Kingdom) for providing the protein V-specific antibody and Ron T. Hay (University of Dundee, Scotland) for the HeLa SUMO cell lines.

S.S. and N.F. were supported by Deutsche Krebsforschung e.V. Part of this work was supported by the Deutsche Forschungsgemeinschaft (SFB TRR179), Else Kröner Fresenius Stiftung, Dräger Stiftung e. V., and the B. Braun Stiftung. The Heinrich Pette Institute, Leibniz Institute for Experimental Virology, is supported by the Freie und Hansestadt Hamburg and the Bundesministerium für Gesundheit.

REFERENCES

1. Berk AJ. 2005. Recent lessons in gene expression, cell cycle control, and cell biology from adenovirus. Oncogene 24:7673–7685. https://doi.org/10.1038/sj.onc.1209040.
2. Lion T. 2014. Adenovirus infections in immunocompetent and immunocompromised patients. Clin Microbiol Rev 27:441–462. https://doi.org/10.1128/CMR.00116-13.
3. Chatterjee PK, Vayda ME, Flint SJ. 1985. Interactions among the three adenovirus core proteins. J Virol 55:379–386.
4. Alestrom P, Akusjarvi G, Lager M, Yeh-kai L, Pettersson U. 1984. Genes encoding the core proteins of adenovirus type 2. J Biol Chem 259:13980–13985.
5. Davison AJ, Benko M, Harrach B. 2003. Genetic content and evolution of adenoviruses. J Gen Virol 84:2895–2908. https://doi.org/10.1099/vir.0.19497-0.
6. Perez-Vargas J, Vaughan RC, Houser C, Hastie KM, Kao CC, Nemerow GR. 2014. Isolation and characterization of the DNA and protein binding activities of adenovirus core protein V. J Virol 88:9287–9296. https://doi.org/10.1128/JVI.00935-14.
7. Matthews DA. 2001. Adenovirus protein V induces redistribution of nucleolin and B23 from nucleolus to cytoplasm. J Virol 75:1031–1038. https://doi.org/10.1128/JVI.75.2.1031-1038.2001.
8. Matthews DA, Russell WC. 1998. Adenovirus core protein V is delivered by the invading virus to the nucleus of the infected cell and later in infection is associated with nucleoli. J Gen Virol 79:1671–1675. https://doi.org/10.1099/0022-1317-79-7-1671.
9. Puntener D, Engelke MF, Ruzsics Z, Strunze S, Wilhelm C, Greber UF. 2011. Stepwise loss of fluorescent core protein V from human adenovirus during entry into cells. J Virol 85:481–496. https://doi.org/10.1128/JVI.01571-10.
10. Hindley CE, Lawrence FJ, Matthews DA. 2007. A role for transportin in the nuclear import of adenovirus core proteins and DNA. Traffic 8:1313–1322. https://doi.org/10.1111/j.1600-0854.2007.00618.x.
11. Bernardi R, Pandolfi PP. 2007. Structure, dynamics and functions of promyelocytic leukaemia nuclear bodies. Nat Rev Mol Cell Biol 8:1006–1016. https://doi.org/10.1038/nrm2277.
12. Tatham MH, Jaffray E, Vaughan OA, Desterro JM, Botting CH, Naismith JH, Hay RT. 2001. Polymeric chains of SUMO-2 and SUMO-3 are conjugated to protein substrates by SAE1/SAE2 and UBC9. J Biol Chem 276:35368–35374. https://doi.org/10.1074/jbc.M104214200.
13. Chu Y, Yang X. 2011. SUMO E3 ligase activity of TRIM proteins. Oncogene 30:1108–1116. https://doi.org/10.1038/onc.2010.462.
14. Spector DL, Ochs RL, Busch H. 1984. Silver staining, immunofluorescence, and immunoelectron microscopic localization of nucleolar phosphoproteins B23 and C23. Chromosoma 90:139–148. https://doi.org/10.1007/BF00292451.
15. Hannoun Z, Maarifi G, Chelbi-Alix MK. 2016. The implication of SUMO in intrinsic and innate immunity. Cytokine Growth Factor Rev 29:3–16. https://doi.org/10.1016/j.cytogfr.2016.04.003.
16. Wimmer P, Schreiner S. 2015. Viral mimicry to usurp ubiquitin and SUMO host pathways. Viruses 7:4854–4872. https://doi.org/10.3390/v7092849.
17. Wimmer P, Schreiner S, Dobner T. 2012. Human pathogens and the host cell SUMOylation system. J Virol 86:642–654. https://doi.org/10.1128/JVI.06227-11.
18. Stefl R, Skrisovska L, Allain FH. 2005. RNA sequence- and shape-dependent recognition by proteins in the ribonucleoprotein particle. EMBO Rep 6:33–38. https://doi.org/10.1038/sj.embor.7400325.
19. Berlow RB, Dyson HJ, Wright PE. 2015. Functional advantages of dynamic protein disorder. FEBS Lett 589:2433–2440. https://doi.org/10.1016/j.febslet.2015.06.003.
20. Wright PE, Dyson HJ. 2015. Intrinsically disordered proteins in cellular signalling and regulation. Nat Rev Mol Cell Biol 16:18–29. https://doi.org/10.1038/nrm3920.
21. Chatterjee PK, Vayda ME, Flint SJ. 1986. Identification of proteins and protein domains that contact DNA within adenovirus nucleoprotein cores by ultraviolet light crosslinking of oligonucleotides 32P-labelled in vivo. J Mol Biol 188:23–37. https://doi.org/10.1016/0022-2836(86)90477-8.
22. Suomalainen M, Greber UF. 2013. Uncoating of non-enveloped viruses. Curr Opin Virol 3:27–33. https://doi.org/10.1016/j.coviro.2012.12.004.
23. Weber JM, Khittoo G. 1983. The role of phosphorylation and core protein V in adenovirus assembly. J Gen Virol 64:2063–2068. https://doi.org/10.1099/0022-1317-64-9-2063.

24. Avgousti DC, Herrmann C, Kulej K, Pancholi NJ, Sekulic N, Petrescu J, Molden RC, Blumenthal D, Paris AJ, Reyes ED, Ostapchuk P, Hearing P, Seeholzer SH, Worthen GS, Black BE, Garcia BA, Weitzman MD. 2016. A core viral protein binds host nucleosomes to sequester immune danger signals. Nature 535:173–177. https://doi.org/10.1038/nature18317.
25. Ugai H, Borovjagin AV, Le LP, Wang M, Curiel DT. 2007. Thermostability/infectivity defect caused by deletion of the core protein V gene in human adenovirus type 5 is rescued by thermo-selectable mutations in the core protein X precursor. J Mol Biol 366:1142–1160. https://doi.org/10.1016/j.jmb.2006.11.090.
26. Ugai H, Dobbins GC, Wang M, Le LP, Matthews DA, Curiel DT. 2012. Adenoviral protein V promotes a process of viral assembly through nucleophosmin 1. Virology 432:283–295. https://doi.org/10.1016/j.virol.2012.05.028.
27. Samad MA, Komatsu T, Okuwaki M, Nagata K. 2012. B23/nucleophosmin is involved in regulation of adenovirus chromatin structure at late infection stages, but not in virus replication and transcription. J Gen Virol 93:1328–1338. https://doi.org/10.1099/vir.0.036665-0.
28. Grisendi S, Mecucci C, Falini B, Pandolfi PP. 2006. Nucleophosmin and cancer. Nat Rev Cancer 6:493–505. https://doi.org/10.1038/nrc1885.
29. Subong EN, Shue MJ, Epstein JI, Briggman JV, Chan PK, Partin AW. 1999. Monoclonal antibody to prostate cancer nuclear matrix protein (PRO:4-216) recognizes nucleophosmin/B23. Prostate 39:298–304. https://doi.org/10.1002/(SICI)1097-0045(19990601)39:4<298::AID-PROS11>3.0.CO;2-M.
30. Tatham MH, Rodriguez MS, Xirodimas DP, Hay RT. 2009. Detection of protein SUMOylation in vivo. Nat Protoc 4:1363–1371. https://doi.org/10.1038/nprot.2009.128.
31. Wimmer P, Berscheminski J, Blanchette P, Groitl P, Branton PE, Hay RT, Dobner T, Schreiner S. 2016. PML isoforms IV and V contribute to adenovirus-mediated oncogenic transformation by functionally inhibiting the tumor-suppressor p53. Oncogene 35:69–82. https://doi.org/10.1038/onc.2015.63.
32. Groitl P, Dobner T. 2007. Construction of adenovirus type 5 early region 1 and 4 virus mutants. Methods Mol Med 130:29–39.
33. Burck C, Mund A, Berscheminski J, Kieweg L, Muncheberg S, Dobner T, Schreiner S. 2015. KAP1 is a host restriction factor that promotes human adenovirus E1B-55K SUMO modification. J Virol 90:930–946. https://doi.org/10.1128/JVI.01836-15.
34. Schreiner S, Bürck C, Glass M, Groitl P, Wimmer P, Kinkley S, Mund A, Everett RD, Dobner T. 2013. Control of human adenovirus type 5 (Ad5) gene expression by cellular Daxx/ATRX chromatin-associated complexes. Nucleic Acids Res 41:3532–3550. https://doi.org/10.1093/nar/gkt064.
35. Sarnow P, Hearing P, Anderson CW, Reich N, Levine AJ. 1982. Identification and characterization of an immunologically conserved adenovirus early region 11,000 Mr protein and its association with the nuclear matrix. J Mol Biol 162:565–583. https://doi.org/10.1016/0022-2836(82)90389-8.
36. Marton MJ, Baim SB, Ornelles DA, Shenk T. 1990. The adenovirus E4 17-kilodalton protein complexes with the cellular transcription factor E2F, altering its DNA-binding properties and stimulating E1A-independent accumulation of E2 mRNA. J Virol 64:2345–2359.
37. Kzhyshkowska J, Kremmer E, Hofmann M, Wolf H, Dobner T. 2004. Protein arginine methylation during lytic adenovirus infection. Biochem J 383:259–265. https://doi.org/10.1042/BJ20040210.
38. Reich NC, Sarnow P, Duprey E, Levine AJ. 1983. Monoclonal antibodies which recognize native and denatured forms of the adenovirus DNA-binding protein. Virology 128:480–484. https://doi.org/10.1016/0042-6822(83)90274-X.
39. Harlow E, Franza BR, Jr, Schley C. 1985. Monoclonal antibodies specific for adenovirus early region 1A proteins: extensive heterogeneity in early region 1A products. J Virol 55:533–546.
40. Lomonosova E, Subramanian T, Chinnadurai G. 2005. Mitochondrial localization of p53 during adenovirus infection and regulation of its activity by E1B-19K. Oncogene 24:6796–6808. https://doi.org/10.1038/sj.onc.1208836.
41. Kindsmüller K, Groitl P, Härtl B, Blanchette P, Hauber J, Dobner T. 2007. Intranuclear targeting and nuclear export of the adenovirus E1B-55K protein are regulated by SUMO1 conjugation. Proc Natl Acad Sci U S A 104:6684–6689. https://doi.org/10.1073/pnas.0702158104.
42. Qiagen. 2016. QIAamp DNA mini and blood mini handbook, 5th ed. Qiagen, Hilden, Germany.